Internal Cancellation of Electric Field Induced Second Harmonic Generation in Solvent Mixtures and Solutions: An Efficient Protocol for the Determination of Molecular Hyperpolarizability

D. Narayana Rao,*,† N. K. M. Naga Srinivas,† P. Gangopadhyay,‡ and T. P. Radhakrishnan*,‡

School of Physics and School of Chemistry, University of Hyderabad, Hyderabad 500 046, India

Received: November 27, 2003; In Final Form: April 21, 2004

Electric field induced second harmonic generation (EFISHG) is a standard technique for the experimental determination of molecular hyperpolarizability. We have developed a novel cell design for EFISHG experiments that makes use of a conventional spectrometer glass cuvette. An efficient and convenient protocol is developed for the analysis of the EFISHG data making use of the internal cancellation of second harmonic generation in solvent mixtures and solutions to determine the first hyperpolarizability value. Calibration experiments and measurements on 4-nitroaniline in DMSO and NMP are presented. The first hyperpolarizability of the zwitterionic push−pull molecule, DCNQI, is measured in DMSO and NMP.

Introduction

Quantitative estimation of the first hyperpolarizability, β, is a critical step in the development of novel molecular systems for quadratic nonlinear optical applications. Electric field induced second harmonic generation (EFISHG) experiments have been widely used for the measurement of β.[1−8] Gases, liquids, and solutions are centrosymmetric ($\chi^{(2)} = 0$) and do not produce second harmonic generation (SHG). However, if the molecules possess a permanent dipole moment μ, they can be partially aligned (limited by thermal fluctuations) by an applied electric field E_0. In an EFISHG experiment the symmetry is broken by the application of an external pulsed dc electric field, allowing the production of second harmonic (2ω) signal when illuminated with a laser of frequency ω; the frequency doubling process is coherent and phase sensitive. Dispersion in the refractive index of the liquid or solution causes the phase velocities of the fundamental and second harmonic waves within the medium to be different. This leads to interference between the "bound" (phase velocity corresponding to ω) and "free" (phase velocity corresponding to 2ω) second harmonic waves.[3] If the path length through the sample is varied, a periodically varying second harmonic signal, the Maker fringe,[9] is obtained. Because EFISHG is a third-order nonlinear process, the second hyperpolarizability, γ, as well as the product, $\mu\beta$, contribute to the SHG. If the applied field and the molecular dipoles are aligned along the *z*-axis, assuming Kleinman[10] symmetry, the quantity measured is

$$\beta_z = \beta_{zzz} + \beta_{zxx} + \beta_{zyy}$$

β_z is the vectorial projection of the hyperpolarizability tensor components β_{ijk} along the direction of the permanent dipole moment. EFISHG does not provide the independent β tensor elements; however, for most of the dipolar organic molecules, the value of β_z represents the dominant component.

Since the early reports[1−6] of EFISHG experiments, several studies have appeared in the literature on the measurements of β of a wide variety of compounds. In principle, EFISHG measurements are capable of yielding precise values of β. However, literature values vary widely for a given compound.[11−13] These variations may arise due to complications in the measurements of the nonlinear optical response, dielectric constant, density, and refractive index of solutions made from different solvents covering a wide range of concentrations.[14,15] These effects are particularly dominant when the measurements are carried out in concentrated solutions. The variations may also arise due to the following factors: the choice of the external absolute reference,[16,17] the shape and the width of the dc electric field pulse used in the experiment, the temporal overlap between the dc and optical pulses,[18] the long path the beam travels inside the conventional cell,[5] the choice of local field factor models,[5,15,19] the data reduction schemes[14−16] and the dipole moment measurements.[20,21] Moreover, error values for the measured β are not always reported. Considerable effort has been made to improve the reproducibility of the results; these include corrections for multiple reflection and finite beam width[22] as well as solvent and cell contributions to the signal.[7,23,24] In view of this scenario, there is significant scope for developing a compact and simple cell design, an easy and straightforward calibration technique preferably using the SHG signal from the solvent itself as a reference and a convenient data analysis protocol, to achieve standardized estimation of β. Our efforts in this direction are described in this paper. The basic theory is reviewed followed by our analysis protocol based on the internal cancellation of the SHG from the two components of binary mixtures. It may be noted that the principle of internal cancellation is implicit in some of the experiments reported by Ledoux and Zyss;[25] we have developed this into a systematic practical tool. The experimental details including a novel and convenient cell design and choice of solvents are described. The calibration experiments and measurements on a push−pull zwitterionic molecule are presented.

* Corresponding author. E-mail: D.N.R., dnrsp@uohyd.ernet.in; T.P.R., tprsc@uohyd.ernet.in.
† School of Physics.
‡ School of Chemistry.

10.1021/jp037635f CCC: $27.50
Published on Web 05/25/2004

Theory and Analysis Protocol

The theoretical background of EFISHG has been discussed extensively in the literature. We present a brief overview pertinent to the present work. The expression for the intensity, $I_{2\omega}^{\mathrm{EFISH}}$ may be written as follows.[8,26]

$$I_{2\omega}^{\mathrm{EFISH}} = k_{\mathrm{inst}}\left|\left(-\frac{\chi_l}{\Delta\epsilon_l}\right)F(e^{-\alpha_{2\omega}L/2} - e^{i\phi(L)})\right|^2 I_\omega{}^2 E_0 \qquad (1)$$

The subscript l refers to the test liquid. k_{inst} is the instrument constant, χ_l is the nonlinear susceptibility, F is the product of different Fresnel factors,[26] and $\alpha_{2\omega}$ is the absorption coefficient of the liquid at the second harmonic frequency. I_ω is the input laser intensity, E_0 is the dc electric field applied, $\Delta\epsilon_l = (n_{2\omega}{}^2 - n_\omega{}^2)_l$ is the dielectric constant dispersion, and $\phi(L) = (\lambda/2L)(n_{2\omega} - n_\omega)_l$ is a periodic phase factor. As the cell is translated vertically, the path length, L, inside the cell changes, causing the oscillation in the second harmonic signal. For nonabsorbing solutions, $\alpha_{2\omega} = 0$ and eq 1 represents an oscillating signal, $|(1 - e^{i\phi(L)})|^2$, giving rise to the characteristic EFISHG Maker fringes with zero minima. For strongly absorbing solutions $e^{-\alpha_{2\omega}L/2} \rightarrow 0$, resulting in a constant value of $I_{2\omega}^{\mathrm{EFISH}}$ for all values of L.

The SHG intensity and the coherence length can be determined from the nonlinear least-squares fit of the Maker fringe trace to the equation

$$I_{2\omega}^{\mathrm{EFISH}} = A_1 \sin^2\left(\frac{\pi x}{A_3} + A_4\right) + A_2 \qquad (2)$$

where x is the cell translation and the fitting parameters A_1, A_2, A_3, and A_4 are the amplitude, intensity offset, periodicity, and an arbitrary phase factor, respectively. A_3 is related to the coherence length by, $l_C = (1/2)A_3 \tan\theta$, where θ is the wedge angle in the cell. The magnitude of A_2 is very small compared to A_1 and is mostly dependent on the beam spot size. The SHG intensity is provided by the value $A_{2\omega}$, defined as $(0.5A_1 + A_2)$. For molecules used in the present study, the absorption limit, $\lambda_{\mathrm{cutoff}}$ is well below the harmonic wavelength. The refractive indices (n_ω and $n_{2\omega}$) and the local field factors of the solvent and solutions are generally quite similar in the dilute regime; under this condition when the solvent and solute molecules do not have any strong interactions, the solution SHG arises from the additive contributions of the solute and the solvent. Based on eq 1, the ratio of the SHG intensities of solution to that of the solvent can be expressed as

$$\left(\frac{A_{2\omega}^{\mathrm{sn}}}{A_{2\omega}^{\mathrm{sv}}}\right)^{1/2} = \pm\left(\frac{\chi_{\mathrm{sn}}}{\chi_{\mathrm{sv}}}\right) = \pm\left(\frac{\chi_{\mathrm{sv}} + \chi_{\mathrm{st}}}{\chi_{\mathrm{sv}}}\right) \qquad (3)$$

The subscripts "sn", "st", and "sv" refer to the solution, solute, and solvent, respectively. For most organic push−pull molecules, the contribution of the third-order term, γ, to the nonlinear susceptibility is much smaller than that from the second-order term, β. The effective nonlinear susceptibility can then be shown to behave as[3] $\chi \propto (N\mu\beta/5k_BT)$.

Equation 3 can therefore be rewritten as

$$\left(\frac{A_{2\omega}^{\mathrm{sn}}}{A_{2\omega}^{\mathrm{sv}}}\right)^{1/2} = \pm\left(1 + \frac{N_{\mathrm{st}}\mu_{\mathrm{st}}\beta_{\mathrm{st}}}{N_{\mathrm{sv}}\mu_{\mathrm{sv}}\beta_{\mathrm{sv}}}\right) \qquad (4)$$

It is convenient to rewrite eq 4 as

$$\left(\frac{A_{2\omega}^{\mathrm{sn}}}{A_{2\omega}^{\mathrm{sv}}}\right)^{1/2} = \pm\left(1 + \frac{\mu_{\mathrm{st}}\beta_{\mathrm{st}}}{k_{\mathrm{sv}}}C_{\mathrm{st}}\right) \qquad (5)$$

C_{st} is the molar concentration of the solute. $k_{\mathrm{sv}} = N_{\mathrm{sv}}\mu_{\mathrm{sv}}\beta_{\mathrm{sv}}/N_A$ is a measure of the nonlinearity exhibited by the solvent in the dilute regime; we call it the "solvent factor". N_{sv} is the number density of the solvent (nearly a constant in dilute solutions) and N_A is the Avogadro number. Equation 5 shows that the plot of $(A_{2\omega}^{\mathrm{sn}}/A_{2\omega}^{\mathrm{sv}})^{1/2}$ against C_{st} would yield a straight line from which the $\mu\beta$ product for the solute can be estimated using k_{sv} and the absolute value of slope, m. We adopt the convention of always plotting the positive value of $(A_{2\omega}^{\mathrm{sn}}/A_{2\omega}^{\mathrm{sv}})^{1/2}$ by choosing the appropriate sign on the right-hand side of eq 5. This leads to line segments with positive and negative y-intercepts, respectively, at the lower and higher regimes of C_{st} from which $\mu_{\mathrm{st}}\beta_{\mathrm{st}}$ can be determined.

$$\mu_{\mathrm{st}}\beta_{\mathrm{st}} = k_{\mathrm{sv}}m \qquad (\text{when intercept is } +1)$$
$$\mu_{\mathrm{st}}\beta_{\mathrm{st}} = k_{\mathrm{sv}}(-m) \qquad (\text{when intercept is } -1) \qquad (6)$$

The hyperpolarizability of the solvent has to be determined from calibration experiments or previous data. The dipole moments of the solvent and solute can be experimentally determined or computed using standard quantum chemical methods.

Total Internal Cancellation. For a specific solute, if the solvent is so chosen that the directions of their $\mu\beta$ products have opposite signs, the internal cancellation of the second harmonic intensity generated by them would make the measured signal decrease progressively when the concentration of the solute increases from low values. Hence, there should be a concentration, C^{TIC}, where the two contributions will be equal and opposite in direction, resulting in complete cancellation of the second harmonic intensity. C^{TIC} can be determined by extrapolation of the data at the lower as well as the higher concentrations. This eliminates the need to record the data near this point, where the SHG signals are often submerged in the noise. At C^{TIC}, $N_{\mathrm{st}}\mu_{\mathrm{st}}\beta_{\mathrm{st}} = -N_{\mathrm{sv}}\mu_{\mathrm{sv}}\beta_{\mathrm{sv}}$. Therefore, the $\mu_{\mathrm{st}}\beta_{\mathrm{st}}$ may also be estimated from

$$\mu_{\mathrm{st}}\beta_{\mathrm{st}} = -\frac{k_{\mathrm{sv}}}{C^{\mathrm{TIC}}} \qquad (7)$$

On the basis of the convention of plotting described above, at $C_{\mathrm{st}} > C^{\mathrm{TIC}}$ a rise in signal is expected. We have determined β_{st} from extrapolated C^{TIC} as well as the slope of the $(A_{2\omega}^{\mathrm{sn}}/A_{2\omega}^{\mathrm{sv}})^{1/2}$ versus concentration plots. Estimations using data close to the pure solvent are expected to parallel the traditional infinite dilution extrapolation procedures.[5] The internal cancellation protocol offers a choice of conditions to evaluate the hyperpolarizability, including the low-concentration, high-concentration, and internal cancellation regimes facilitating a deeper understanding of intermolecular interactions. For example, absence of solute−solute interactions over the full range of concentrations will be reflected in perfectly linear variation of the data points with similar slopes on either side of the C^{TIC}.

Experimental Method

Design of the Cell. The sample cell design is a key factor in the EFISHG experiment. It is important to have a uniform field applied to the liquid sample. The well-established approach is to construct a cell with a wedge-shaped space where the liquid resides, bounded by sharp boundaries. In most of the designs, the wedge is translated in a direction perpendicular to the

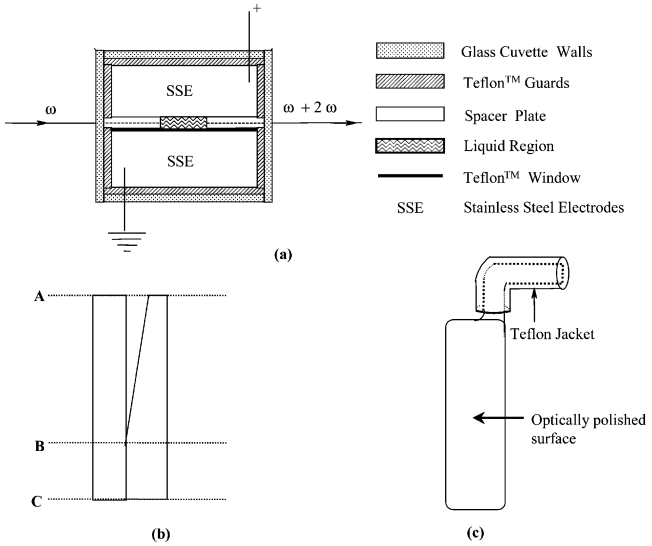

Figure 1. Cell design for EFISHG measurements: (a) top view of the cell assembly; (b) side view of the spacer glass plates (AB: Liquid in the wedge region, BC: No-liquid region); (c) stainless steel electrode.

incident fundamental beam. Dworczak and Keislinger[24] have reviewed the various cells reported in the literature. We describe below the cell we have designed.

The cell is assembled inside a standard spectroscopic glass cuvette (Model 3070-OG-10, Hellma, Germany) having inner dimension 9.9 × 9.2 × 45 mm^3. Two optically polished BK7 glass plates (1.1 mm thick) were used to construct the wedge; we refer to them as the spacer plates. One of these plates has a wedge shaped cut with an angle of 2.56°. They are held in the central region of the cell by the optically polished stainless steel electrodes and the Teflon guards placed on the sides. The top view of the cell is depicted in Figure 1a. The Teflon guards prevent electric discharge between the electrodes. Further protection is provided by a thin (200 μm) Teflon frame with a wedge-shaped window inserted between the glass spacer and the grounded electrode. This Teflon spacer enabled the application of high voltage over the short interelectrode distance, which in our cell is 1.3 mm. To the best of our knowledge, this is one of the shortest interelectrode distances used in an EFISHG cell. The straight regions (within BC in Figure 1b) of the spacer plates are under the field but do not contain any liquid between. This region facilitates the monitoring of possible contribution to the EFISHG signal from the glass; under our experimental conditions no detectable SHG was observed from the glass spacers or the cell walls. The electrodes and glass spacers allow a wedge-shaped liquid film to form in the middle of the cell (within AB in Figure 1b) with a total volume of approximately 0.5 mL. The fundamental beam enters the cell from the side having the straight cut glass spacer. The beam travels through the optically polished faces of the spacer plates. Because no liquid enters between the spacer glass plates and the cell wall and practically the whole bulk of the liquid resides in the wedge space, the effect of beam diameter on fringe contrast is markedly less in our cell compared to other wedge cells.

EFISHG Experiment. The setup for our EFISHG measurements follows standard practice (Figure 2). A Q-switched Nd:YAG laser was used as the source of the linearly polarized fundamental radiation at 1064 nm. The laser (Spectra-Physics; Model INDI 40) delivered pulses with maximum power of 495 mJ and 6 ns duration with a repetition rate of 10 Hz. Variation of peak power was <3% with a beam divergence <0.8 mrad. The diameter of the laser beam was limited to 4 mm by a hard

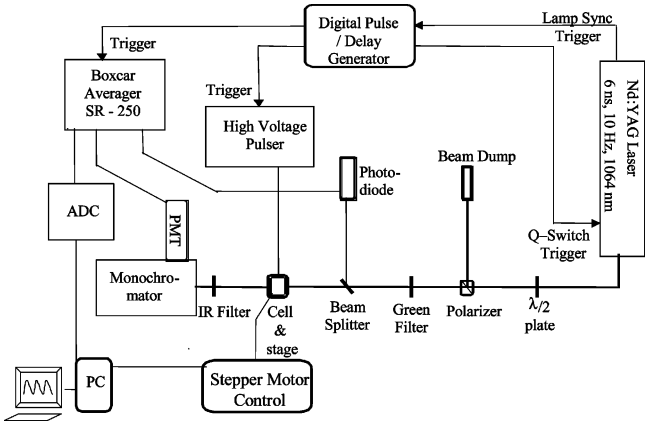

Figure 2. Experimental setup for the EFISHG measurement.

aperture. Four percent of this beam was reflected, passed through appropriate optics, and focused loosely onto the cell. The beam intensity was tuned using a half-wave plate and polarizing beam splitter combination. The linearly polarized part was passed through an IR pass filter and focused using a 35 cm lens, thus providing a beam with a waist of 120 μm at focus and a Rayleigh range of 40 mm. The cell assembly is fixed on a homemade polypropylene mount that could be translated vertically using computer-controlled stepping motors (Dynalog Microsystems Pvt. Ltd.,; Model PCL 812) with a resolution of 5 μm. The wedge-shaped glass spacer allows the path length of the beam in the solution to be varied from 0 to 1.9 mm over a vertical translation of 33.4 mm. Voltage pulses were applied to the electrodes using a high power pulse generator (Velonex; Model 345). A digital delay/pulse generator (Stanford Research Systems Inc.; Model DG 535) was used to synchronize the firing of the Q-switch of the laser, the high voltage pulser and the boxcar averager. The peak voltage is set to 6.0 kV with a pulse width of 1.5 μs at half amplitude. This voltage effectively provides a field of 4.62 MV m^{-1} on the sample. Four percent of the main beam split before focusing onto the cell and detected by a photodiode is used as a reference to monitor the pulse-to-pulse fluctuations in the laser beam. The second harmonic generated from the EFISHG cell is collected using appropriate optics, passed through an IR filter, and focused onto the monochromator, set for 532 nm. The signal from the monochromator is collected using a photomultiplier tube (Hamamatsu 230) and preamplifier (Stanford Research Systems Inc.; Fast Preamp Model SRS 240). Both reference and the signal are sampled and averaged simultaneously in a boxcar averager (Stanford Research Systems Inc.; Model SR250), collected, and processed on a personal computer. The cell position is moved in 20 μm increments to collect the data points for the fringe. Before each data collection, background noise was collected for both signal and reference and used to correct the experimental data.

The solvents used in the experiment are freshly dried (over calcium oxide) and vacuum distilled at least twice before use. The solutes (Figure 3) are purified using multiple crystallization or sublimation and dried under dynamic vacuum. The solutions are filtered using a 0.2 μm PTFE filter (Millipore; Model FGLP 013 00 FG). After each data collection the cell is unpacked and all components washed and dried. Variations between different packings of a given solution were negligible.

Choice of Solvents. A considerable part of the EFISHG signal originates from the solvent. Many of the compounds of interest for SHG applications are the so-called push−pull molecules, which generally are quite polar. Diaminodicyanoquinodimethane

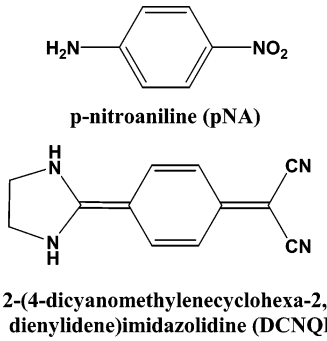

Figure 3. Molecules considered in this study.

TABLE 1: Boiling Point (bp), Refractive Index (n_D^{20}), Dielectric Constant (ϵ), Dipole Moment (μ), and Solvent Factor (k_{sv}) of *N*-Methyl-2-pyrrolidinone (NMP) and Dimethyl Sulfoxide (DMSO)

solvent	bp (°C)	n_D[a]	ϵ[b]	μ (D)[b]	$10^{48}k_{sv}$ (M esu)
NMP	202	1.488	32.0	4.09	10.481 ± 1.781[c]
DMSO	198	1.479	46.7	4.10	-10.978 ± 1.647[d]

[a] References 35, 36, and 37. [b] References 35 and 36. [c] This work. [d] Using β from ref 25.

derivatives, which we have been investigating,[27−29] are typical examples, possessing very large dipole moments in the range 15−45 D.[30−33] Such molecules generally do not dissolve in low-polarity solvents such as 1,4-dioxane and benzene and are known to aggregate in solvents such as chloroform.[34] We have therefore chosen to use *N*-methyl-2-pyrrolidinone (NMP) and dimethyl sulfoxide (DMSO) as solvents for our experiments. These solvents have appreciable $\mu\beta$ values of opposite sign (Table 1) and serve as convenient internal references for molecules possessing large nonlinearities. They have several other advantages as well. Being highly polar, these solvents are capable of dissolving most of the materials of interest in quadratic NLO applications, unlike chloroform and 1,4-dioxane. The high polarity of these solvents discourages aggregate formation of polar solute molecules. The refractive indices are close to that of glass (BK7), reducing the walk-off of the beam inside the cell, which is of considerable importance because the interelectrode distance in our cell is relatively short. Finally, the high boiling points of these solvents suit very well their use in our miniature open cell, with negligible evaporation problem.

DMSO is used as the primary internal reference in our EFISHG experiments. Thus it is important that correct values of its dipole moment and hyperpolarizability are used. The reported values of μ_{DMSO} range from 3.9 to 4.3 D. We have chosen to use the most commonly used and recent value of 4.1 D.[35,36] Two rather different values have been reported for β_{DMSO}, $-(0.07 \pm 0.01) \times 10^{-30}$ esu[14] and -0.19×10^{-30} esu.[25] We have chosen the latter value in all our experiments; the justification for this comes from the study carried out on the prototypical molecule, 4-nitroaniline described later. The physical constants of interest for NMP and DMSO are collected in Table 1; it may be noted that the k_{sv} of NMP is based on the β measured in this study.

Results and Discussion

First Hyperpolarizability of *N*-Methyl-2-pyrrolidinone (NMP). From the study of 4-nitroaniline by Stähelin et al.[38] one can infer that the $\mu\beta$ of NMP is positive. However, to the best of our knowledge β_{NMP} has not been reported. As an illustration of our methodology, we have determined β_{NMP} using

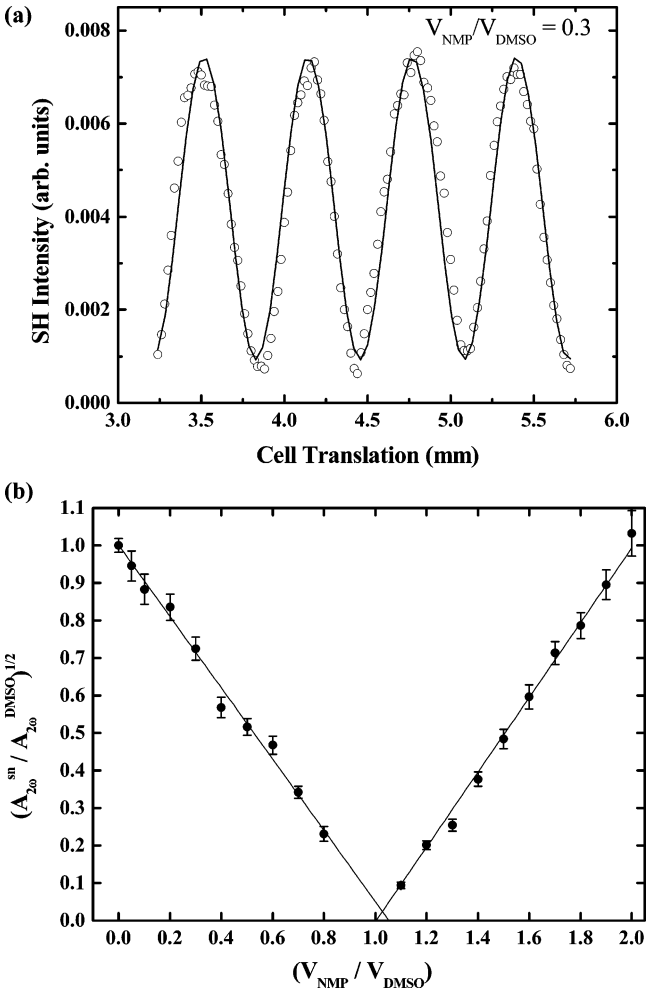

Figure 4. (a) Maker fringes recorded for NMP in DMSO solution (volume ratio of 0.3). (b) Plot of $(A_{2\omega}^{sn}/A_{2\omega}^{sv})^{1/2}$ against (V_{NMP}/V_{DMSO}) for NMP−DMSO.

the NMP−DMSO liquid mixture. For the NMP−DMSO mixture it is convenient to rewrite eq 4 in terms of volume ratios as

$$\left(\frac{A_{2\omega}^{sn}}{A_{2\omega}^{sv}}\right)^{1/2} = \pm\left[1 + \left(\frac{\rho_{NMP}/M_{NMP}}{\rho_{DMSO}/M_{DMSO}}\right)\left(\frac{\mu_{NMP}\beta_{NMP}}{\mu_{DMSO}\beta_{DMSO}}\right)\left(\frac{V_{NMP}}{V_{DMSO}}\right)\right] \quad (8)$$

where ρ and M are the density and the molecular weight, respectively, and V denotes the volume of each liquid taken to form the mixture.

A typical Maker fringe recorded for NMP−DMSO is shown in Figure 4a. The EFISHG signal intensity as a function of the volume ratios is shown in Figure 4b. Because the $\mu\beta$ of DMSO and NMP possess opposite signs, as discussed earlier, the signal decreases as the concentration is increased from low values and increases at higher values. The slope of the line on the left-hand side of C^{TIC} is -(0.9498 ± 0.0175) whereas the slope on the right is +(0.9969 ± 0.0043). The volume ratio at the point of total internal cancellation obtained by extrapolation of the lines on the left and right-hand sides are respectively 1.053 ± 0.0194 and 1.003 ± 0.0043. β_{NMP} is estimated (Table 2) using the slopes as well as the C^{TIC} and $\mu\beta$ value of DMSO and μ of NMP. β_{1064} estimated from the low- and high-concentration regions are the same within the error limits. However, for reasons noted earlier, we chose the value obtained from the slope

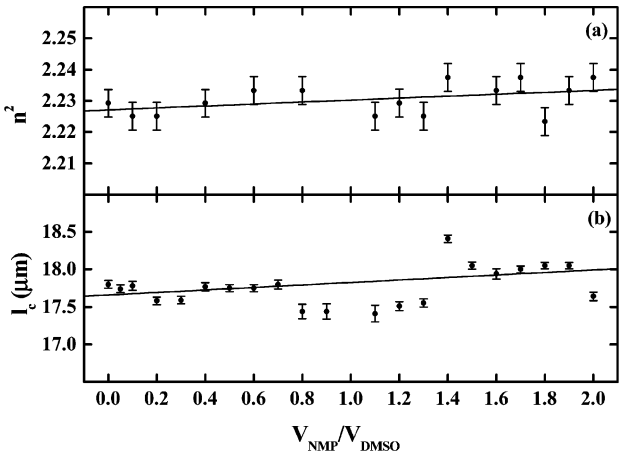

Figure 5. (a) Square of the refractive index (n^2) and (b) coherence length (l_c) for the NMP−DMSO mixtures plotted against the volume ratios.

TABLE 2: First Hyperpolarizability at 1064 nm (β_{1064}) of *N*-Methyl-2-pyrrolidinone (NMP)

	$10^{30}\beta_{1064}$ (esu)	
	using slope	using C^{TIC} from extrapolation
left-hand side	0.25 ± 0.04	0.25 ± 0.04
right-hand side	0.26 ± 0.04	0.26 ± 0.04

of the line in the lower concentration region, (0.25 ± 0.04) × 10^{-30} esu, as the standard value for further experiments. Routine estimation of β may be carried out using measurements in the lower concentration regime alone.

The coherence length estimated from the EFISHG data for the NMP−DMSO mixtures are plotted against the volume ratios in Figure 5. The figure also shows the square of the refractive indices measured[39] for the various mixtures. The plots show very little variation in the values across the different compositions, justifying the assumptions made earlier.

First Hyperpolarizability of 4-Nitroaniline (pNA) and 2-[4-(Dicyanomethylene)cyclohexa-2,5-dienylidene]imidazolidine (DCNQI). pNA is known to have a positive β; values ranging from 17 × 10^{-30} to 47 × 10^{-30} esu have been reported depending on the solvent used. To the best of our knowledge, EFISHG measurement of β of pNA in DMSO has not been reported. However, β_{pNA} in DMSO has been reported as 28.8 × 10^{-30} esu from an HRS measurement.[40] Our EFISHG experiments on pNA in NMP and DMSO demonstrate clearly the principle of internal cancellation of SHG in solutions. Because the $\mu\beta$ of DMSO and pNA have opposite signs, a C^{TIC} is expected and is observed at 0.035 M. At higher concentrations the second harmonic signal increases. However, in NMP the EFISHG signal increases with the concentration all through. The plot of the SHG intensity against concentration of pNA for the two cases are shown in Figure 6. Once again we have verified that the refractive index and coherence length change little with concentration. β_{pNA} determined in DMSO and NMP solutions are presented in Table 3; in the former case, the values from C^{TIC} as well as from either side of it are provided. The absorption maximum for pNA in DMSO and NMP are 398 and 386 nm, respectively (Figure 7). The static hyperpolarizabilities, β_0, computed from β_{1064} using the dispersion model,[3]

$$\beta_0 = \beta_\omega\left(1 - \frac{\lambda_{max}^2}{\lambda^2}\right)\left(1 - 4\frac{\lambda_{max}^2}{\lambda^2}\right) \qquad (9)$$

are also provided in Table 3.

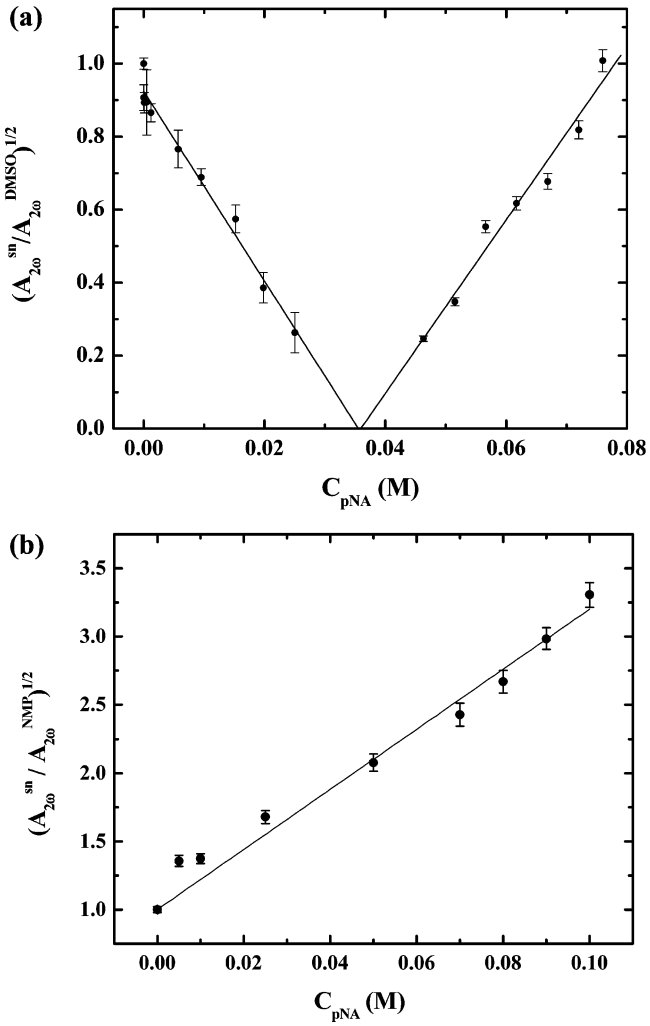

Figure 6. Plot of $(A_{2\omega}^{sn}/A_{2\omega}^{sv})^{1/2}$ against concentration of pNA in (a) DMSO and (b) NMP.

TABLE 3: Dipole Moment (μ), Absorption Maximum (λ_{Max}), First Hyperpolarizability at 1064 nm (β_{1064}), and Static First Hyperpolarizability (β_0) of pNA in DMSO and NMP

solvent	μ (D)	λ_{max} (nm)	$10^{30}\beta_{1064}$ (esu) (reported)	$10^{30}\beta_{1064}$ (esu)	$10^{30}\beta_0$ (esu)
DMSO	6.2[a]	398	28.8[b]	53.54 ± 11.06[c] 50.58 ± 10.17[d] 46.17 ± 7.48[e] 49.18 ± 8.07[f]	20.43 ± 4.9[c]
NMP	6.8[g]	386	38.4[g]	33.94 ± 6.86	13.96 ± 2.82

[a] Reference 37. [b] Reference 40 (β from HRS measurement). [c] Using left-hand side slope. [d] Using C^{TIC} from left-hand side extrapolation. [e] Using right-hand side slope. [f] Using C^{TIC} from right-hand side extrapolation. [g] Reference 38 (β from EFISHG measurement).

Data in Table 3 show that β_{pNA} measured in NMP agrees quite well with the reported value. This provides confidence in the β_{NMP} determined earlier and further suggests that the earlier choice of β_{DMSO} is justified. The positive solvatochromic effect seen in the absorption spectra of pNA in NMP and DMSO is indicative of a positive $\Delta\mu$ on excitation, leading to the positive value of $\mu\beta$. The two-level dispersion model explains the larger β in DMSO. β_0 estimated from the measurements in the two solvents are clearly closer in magnitude.

We have carried out EFISHG measurements on DCNQI, which has been reported to have a large β_{1064} of −(240 ± 60) × 10^{-30} esu.[41] This value was arrived at on the basis of an

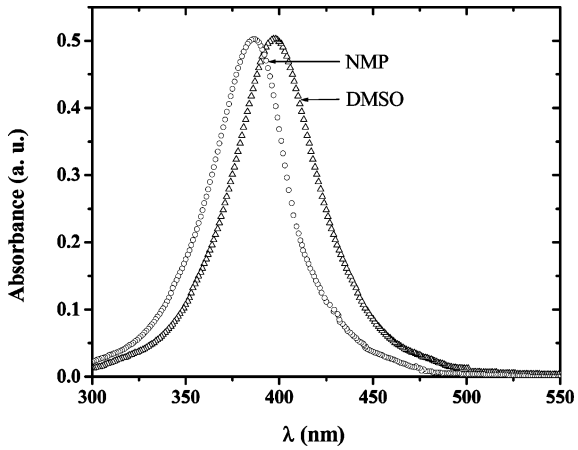

Figure 7. Electronic absorption spectra of pNA in DMSO and NMP.

EFISHG measured $\mu\beta$ of $-(840 \pm 210) \times 10^{-30}$ esu and dipole moment of 3.5 D estimated using an INDO calculation. The computed μ of DCNQI appears to be a gross underestimate in view of the recent measurements on related molecules in solution[30,31] and solid state.[32,33] As in the previous study, we have carried out the experiment in DMSO. Because the experimental value of μ_{DCNQI} is not available, we have calculated it using the AM1 semiempirical method;[42] the solvent environment was simulated by invoking the COSMO subroutine[43] and imposing the dielectric constant of DMSO. Calculation on the fully optimized geometry of DCNQI yielded a value of 30 D; this value appears to be a fair estimate in view of the experimental dipole moment of similar molecules. Because DCNQI and DMSO both possess negative $\mu\beta$, the SHG signal increases with increasing concentration of DCNQI (Figure 8a). The estimated β value is provided in Table 4. Cross et al.[34] have reported the possibility of aggregation of diaminodicyanoquinodimethanes in chloroform. The electronic absorption spectra recorded at similar concentrations of DCNQI in DMSO as used in the EFISHG experiment follow linear behavior; no sign of molecular aggregation is visible. Therefore, DMSO appears to be a better choice for EFISHG experiments on these types of molecules. The data from the EFISHG study of DCNQI in NMP are shown in Figure 8b. Because the $\mu\beta$ products of DCNQI and NMP have opposite sign, a C^{TIC} is observed. The slopes of the left and the right sides of the plot are slightly different. β is estimated using the C^{TIC} as well as the lower and higher concentration regimes (Table 4); μ was again obtained from AM1/COSMO computation imposing the dielectric constant of NMP. As in the case of the DMSO solution, optical absorption spectra in NMP solutions also do not indicate any aggregation even at concentrations as high as 0.016 M.

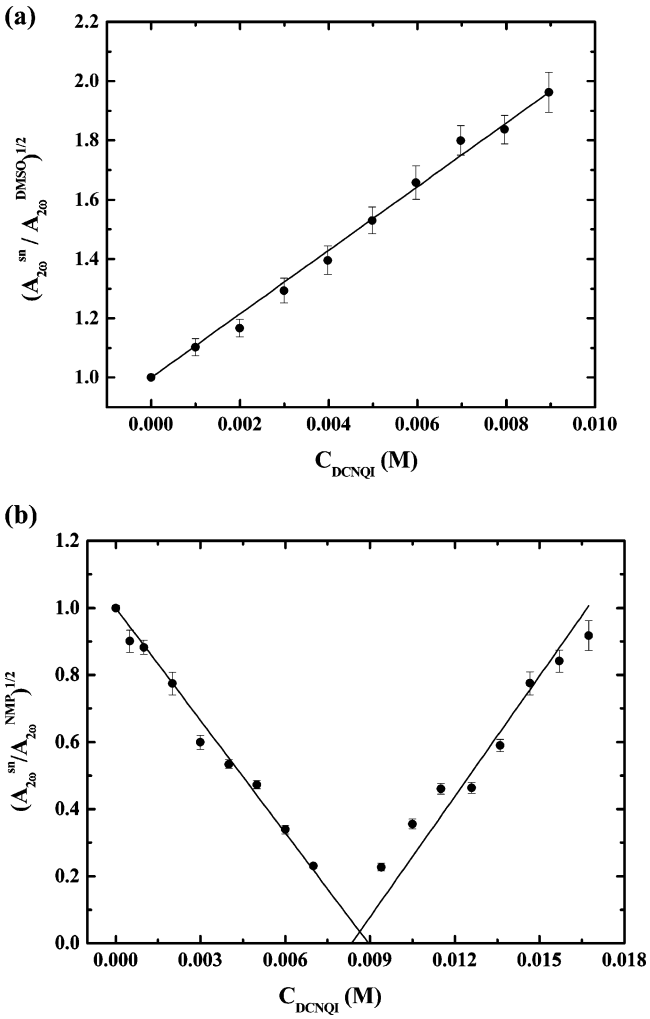

Figure 8. Plot of $(A_{2\omega}^{sn}/A_{2\omega}^{sv})^{1/2}$ against concentration of DCNQI in (a) DMSO and (b) NMP.

TABLE 4: Dipole Moment (μ), Absorption Maximum (λ_{Max}), First Hyperpolarizability at 1064 nm (β_{1064}), and Static First Hyperpolarizability (β_0) of DCNQI in DMSO and NMP

solvent	μ (D)	λ_{max} (nm)	$10^{30}\beta_{1064}$ (esu)	$10^{30}\beta_0$ (esu)
DMSO	30.02	404	-39.30 ± 6.51^a	-14.2 ± 2.36
NMP	31.3	411	-37.44 ± 7.24^b	-12.73 ± 2.46^b
			-37.45 ± 7.22^c	
			-40.11 ± 7.49^d	
			40.09 ± 7.49^e	

[a] The value reported[41] for $\mu\beta_{1064}$ is $-(840 \pm 210) \times 10^{-30}$ esu. [b] Using left-hand side slope. [c] Using C^{TIC} from left-hand side extrapolation. [d] Using right-hand side slope. [e] Using C^{TIC} from right-hand side extrapolation.

Conclusions

We have developed a simple cell design for EFISHG experiments, which uses a standard spectrometer cuvette and as little as 0.5 mL of solutions. Advantages of using DMSO and NMP as solvents for these experiments is demonstrated; they offer the choice of positive and negative $\mu\beta$ values so that NLO-phores with either sign of the $\mu\beta$ can be studied using the internal cancellation method developed here. Our method, like other EFISHG approaches, is applicable only to neutral dipolar molecules. We have presented a convenient analysis protocol for the data. The first hyperpolarizability determined for pNA and DCNQI in DMSO and NMP using our analysis show fair agreement with those reported in the literature. β_{1064} of DCNQI are $-(39.3 \pm 6.51) \times 10^{-30}$ and $-(37.44 \pm 7.24) \times 10^{-30}$ esu, respectively, in the two solvents. The advantages of the internal cancellation procedure are that it facilitates (i) easy and convenient determination of molecular hyperpolarizability, (ii) accurate measurements in the noninteracting regime as done by infinite dilution extrapolation method, and (iii) investigation of NLO-phore interactions in the solution state by experimentation in different concentration regimes.

Acknowledgment. We acknowledge with gratitude the financial support from the Department of Science and Technology, New Delhi (Swarnajayanti Fellowship), and Department of Atomic Energy (BRNS), India.

References and Notes

(1) Levine, B. F.; Bethea, C. G. *J. Chem. Phys.* **1974**, *60*, 3856.
(2) Levine, B. F.; Bethea C. G. *J. Chem. Phys.* **1975**, *63*, 2666.
(3) Oudar, J. L. *J. Chem. Phys.* **1977**, *67*, 446.
(4) Oudar, J. L.; Chemla, D. S. *J. Chem. Phys.* **1977**, *66*, 2664.
(5) Singer, K. D.; Garito A. F. *J. Chem. Phys.* **1981**, *75*, 3572.
(6) Nicoud, J. F.; Twieg, R. J. In *Nonlinear Optical Properties of Organic Molecules and Crystals*; Chemla, D. S., Zyss, J., Eds.; Academic Press: Orlando, 1987; Vol. 1, Chapter II-3, pp 255−267 and Vol. 2, Appendix II, pp 255−267.
(7) Bosshard, C.; Knöpfle, G.; Prêtre, P.; Günter, P. *J. Appl. Phys.* **1992**, *71*, 1594.
(8) (a) Berkovic, G.; Meshulam, G.; Kotler, Z. *J. Chem. Phys.* **2000**, *112*, 3997. (b) Maya, E. M.; García-Frutos, E. M.; Vázquez, P.; Torres, T.; Martín, G.; Rojo, G.; Agulló-López, F.; Gonza'lez-Jonte, R. H.; Ferro, V. R.; de la Vega José, M. G.; Ledoux, I.; Zyss, J. *J. Phys. Chem. A* **2003**, *107*, 2110.
(9) Maker, P. D.; Terhune, R. W.; Niesenoff, M.; Savage, C. M. *Phys. Rev. Lett.* **1962**, *8*, 21.
(10) Kleinman, D. A. *Phys. Rev.* **1962**, *126*, 1977.
(11) Karna, S. P.; Prasad, P. N.; Dupuis, M. *J. Chem. Phys.* **1991**, *94*, 1171.
(12) Mikkelsen, K. V.; Luo, Y.; Agren, H.; Jørgensen, P. *J. Chem. Phys.* **1994**, *100*, 8240.
(13) Wang, C. K.; Wang, Y. H.; Yan, S.; Yi, L. *J. Chem. Phys.* **2003**, *119*, 4409.
(14) Cheng, L. T.; Tam, W.; Stevenson, S. H.; Meredith, G. R.; Rikken, G.; Marder, S. R. *J. Phys. Chem.* **1991**, *95*, 10631.
(15) Cheng, L. T.; Tam, W.; Marder, S. R.; Stiegman, A. E.; Rikken, G.; Spangler, C. W. *J. Phys. Chem.* **1991**, *95*, 10643.
(16) Willets, A.; Rice, J. E.; Burland, D. M.; Shelton, D. P. *J. Chem. Phys.* **1992**, *97*, 7590.
(17) Stähelin, M.; Moylan, C. R.; Burland, D. M.; Willetts, A.; Rice, E. J.; Shelton, D. P.; Donley, E. A. *J. Chem. Phys.* **1993**, *98*, 5595.
(18) Chang, S. L.; Glaser, R.; Sharp, P.; Kauffman, J. F. *J. Phys. Chem. A* **1997**, *101*, 7176.
(19) Meredith, G. R.; Buchalter, B. *J. Chem. Phys.* **1983**, *78*, 1938.
(20) Liu, C. S.; Kauffman, J. F. *Rev. Sci. Instrum.* **1996**, *67*, 525.
(21) Chen, G. S.; Liu, C. S.; Glaser, R.; Kauffman, J. F. *Chem. Commun.* **1996**, *15*, 1719.
(22) Jerphagnon, J.; Kurtz, S. K. *J. Appl. Phys.* **1970**, *41*, 1667.
(23) Heflin, J. R.; Cai, Y. M.; Garito, A. F. *J. Opt. Soc. Am. B* **1991**, *8*, 2132.
(24) Dworczak R.; Keislinger D. *Phys. Chem. Chem. Phys.* **2000**, *2*, 5057.
(25) Ledoux, I.; Zyss, J. *Chem. Phys.* **1982**, *73*, 203.
(26) Kajzar, F.; Ledoux, I.; Zyss J. *Phys. Rev. A* **1987**, *36*, 2210.
(27) Ravi, M.; Radhakrishnan, T. P. *J. Phys. Chem.* **1995**, *99*, 17624.
(28) Ravi, M.; Gangopadhyay, P.; Rao, D. N.; Cohen, S.; Agranat, I.; Radhakrishnan, T. P. *Chem. Mater.* **1998**, *10*, 2371.
(29) Gangopadhyay, P.; Agranat, I.; Rao, D. N.; Radhakrishnan, T. P. *Enantiomer* **2002**, *7*, 119.
(30) Szablewski, M.; Thomas, P. R.; Thornton, A.; Bloor, D.; Cross, G. H.; Cole, J. M.; Howard, J. A. K.; Malagoli, M.; Meyers, F.; Bredas, J.-L.; Wensellers, W.; Goovaerts, E. *J. Am. Chem. Soc.* **1997**, *119*, 3144.
(31) Kagawa, Y.; Szablewski, M.; Ravi, M.; Hackman, N. A.; Cross, G. H.; Bloor, D.; Batsanov, A. S.; Howard, J. A. K. *Nonlinear Opt.* **1999**, *22*, 235.
(32) Gopalan, R. S.; Kulkarni, G. V.; Ravi, M.; Rao, C. N. R. *New J. Chem.* **2001**, *25*, 1108.
(33) Cole, J. M.; Copley, R. C. B.; McIntyre, G. J.; Howard, J. A. K.; Szablewski, M.; Cross, G. H. *Phys. Rev. B* **2002**, *65*, 125107.
(34) Cross, G. H.; Hackman, N.-A.; Thomas, P. R.; Szablewski, M.; Palsson, L.-O.; Bloor, D. *Opt. Mater.* **2002**, *21*, 29.
(35) Riddick, J. A.; Bunger, W. B.; Sakano, T. K. *Organic Solvents*; Wiley: New York, 1986.
(36) Sit, S. K.; Dutta, K.; Acharya, S.; Pal Majumdar, T.; Roy, S. *J. Mol. Liq.* **2000**, *89*, 111.
(37) *CRC Handbook*, 77th ed.; CRC Press: Boca Raton, FL, 1996.
(38) Stähelin, M.; Burland, D. M.; Rice, J. E. *Chem. Phys. Lett.* **1992**, *191*, 245.
(39) Kumar, V. N.; Rao, D. N. *J. Opt. Soc. Am. B* **1995**, *12*, 1559.
(40) Woodford, J. N.; Pauley, M. A.; Wang, C. H. *J. Phys. Chem. A* **1997**, *101*, 1989.
(41) Lalama, S. J.; Singer, K. D.; Garito, A. F.; Desai, K. N. *Appl. Phys. Lett.* **1981**, *39*, 940.
(42) Dewar, M. J. S.; Zoebisch, E. G.; Healy, E. F.; Stewart, J. J. P. *J. Am. Chem. Soc.* **1985**, *107*, 3902. MOPAC2002, Fujitsu Inc.
(43) Klamt, A.; Schüürmann, G. *J. Chem. Soc., Perkin Trans. 2* **1993**, 799.